Journal of the Korean Nuclear Society
Volume 24, Number 3, September 1992

A New Approach for the Solution of Multi-Dimensional Neutron Kinetics Equations in LWR's

Jae Woong Song
Korea Atomic Energy Research Institute

Jong Kyung Kim
Hanyang University

(Received January 22, 1992)

경수로에 대한 다차원 노심 동특성 방정식의 해를 구하기 위한 새로운 방법 개발

송재웅
한국원자력연구소

김종경
한양대학교

(1992. 1. 22 접수)

Abstract

The intent of this study is to develop an efficient calculation method which can be used to analyze the heterogeneous time-dependent reactor problems. By using the nodal theory one can not only reduce the calculational efforts, but accurately determine the group dependent flux densities averaged over the entire homogeneous nodes. This method uses correction factors(called "discontinuity factors") in a rigorous manner to obtain the relationship between the node-averaged flux and the surface-averaged fluxes and currents. The discontinuity factors are calculated from the node-averaged fluxes, diffusion coefficients, and the discontinuity factors of the previous time step. The test results for two benchmark problems demonstrate the accuracy and efficiency of the method developed for the transient application in which assembly-size nodes can be used.

요 약

시간 및 공간 종속형 중성자 수송 방정식으로 부터 비균질 원자로 노심해석의 효율적인 방법을 개발하였다. 이를 위해 계산 시간을 단축하고 각 집합체 크기의 소격격자(coarse mesh)에 대한 평균 중성자속을 정확히 예측할 수 있도록 노달방법(nodal method)을 도입하였고, 노드 별 평균 중성자속과 노드 각 경계면의 평균 중성자속 및 유속(flux and current)과의 관계식을 얻기 위하여 조정인자(correction factor)로서 불연속인자(discontinuity factor)를 사용하였으며, 이 인자는 이전 시간대(previous time step)의 노드 평균 중성자속, 확산계수, 그리고 불연속인자 등에 따라 새로이 계산(updating)된다. 본 논문에서 개발된 방법을 시간에 따라 비교적 단순히 변하는 과도 노

심(TWIGL)과 급격한 중성자 거동의 변화를 모사하는 과도 노심(LRA)에 적용한 결과 정확성 및 효율성이 입증되었다.

1. Introduction

The safe operation of a nuclear reactor requires the fast and accurate determination of the nuclear characteristics for steady state and transient core conditions, and many hypothetical accident scenarios. The investigation of such situations requires calculational tools that can be used for various transient analyses. In a recent year, Werner [1], Finnemann[2], Sims[3], Shober[4], and Smith[5] have solved transient problems using ANM(Analytical Nodal Method), NEM, and Response Matrix Method to get accurate solutions. These methods also reduce much of execution time compared to traditional finite-difference method. Since their formulations were mainly derived from the diffusion equations, the equivalence theory can be introduced to include the transport effects and to predict well the power distributions without leading to large computationally efforts near the severe flux tilt regions.

The intent of this study is to develop an efficient calculation method which can be used to analyze the heterogeneous time-dependent reactor problems. By using the nodal theory, one can not only reduce the calculational efforts, but accurately determine the group dependent flux densities averaged over the entire homogeneous nodes. The nodal balance equations can be derived directly from the Boltzmann transport equation. The difficulty involved with nodal method, however, is in obtaining coupling relations that relate the node-averaged flux and the face-averaged fluxes and currents. The method, which were suggested by Koebke[6], later modified by Smith[7], and applied to static fast reactor problem by Chang[8], does have the ability of reproducing any exact solution. This method uses correction factors(called "discontinuity factors") in rigorous manner to obtain the relationship between the node-averaged flux and the surface-averaged fluxes and currents.

In this study, the method using discontinuity factor will be applied for transient problems to reduce errors coming from the node homogenization and finite-difference method. The method uses a conventional inner and outer iteration schemes. The computer code based on the method is tested and applied to benchmark problems to determine its accurary and efficiency.

2. Theoretical Model

2.1. Derivation of Time-Dependent Nodal Balance Equation

The nodal balance equation, which is directly derived by the time-dependent transport equation with delayed neutrons, for the neutronics behavior of the reactor can be written in standard multi-group form

$$\frac{1}{v_g}\frac{\partial \bar{\phi}_g^{i,j,k}(t)}{\partial t} + \frac{1}{V_{i,j,k}}\sum_{n=1}^{6}\int_{S_n} J_g(\vec{r},t)\cdot\hat{n}_{S_n}dS_n + \Sigma_g^{i,j,k}(t)\,\bar{\phi}_g^{i,j,k}(t)$$
$$= \sum_{g'=1}^{G}\chi_g(1-\beta)\,\nu\Sigma_{fg'}^{i,j,k}(t)\,\bar{\phi}_{g'}^{i,j,k}(t) + \sum_{g'\neq g}\Sigma_{gg'}^{i,j,k}(t)\,\bar{\phi}_{g'}^{i,j,k}(t) + \sum_{d=1}^{DG}\lambda_d\bar{C}_d^{i,j,k}(t) \quad (1)$$

and

$$\frac{\partial \bar{C}_d^{i,j,k}(t)}{\partial t} + \lambda_d\bar{C}_d^{i,j,k}(t) = \beta_d\sum_{g'=1}^{G}\nu\Sigma_{fg'}^{i,j,k}(t)\,\bar{\phi}_{g'}^{i,j,k}(t) \quad (2)$$

The notation is fairly standard, and the double-barred $\bar{\phi}_g^{i,j,k}$ and $C_d^{i,j,k}$ account for the volume-averaged neutron flux and delayed neutron precursor density in node (i,j,k), respectively. The summation $\sum_{n=1}^{6}$ is over all six faces of the mesh cube, the $\hat{n}_{S_n}$ being outward drawn normal to surface S_n. It is assumed that all cross-sections are constant within each node. However, since it in-

volves the surface-averaged net currents and volume-averaged flux, $\bar{\bar{\phi}}_g^{i,j,k}$, further relationship between these unknowns are needed. Fick's law and the finite-difference approximation are accordingly employed in an expression for the surface-averaged net current at a common surface of two adjacent nodes. Thus the surface-averaged net current at x_{i+1} between node (i,j,k) and node (i+1,j,k) as shown in Figure 1 can be written as, for a group g,

$$\bar{J}_g(x_{i+1},t) = \frac{1}{h_y^j h_z^k}\int_{h_y^j} dy \int_{h_z^k} dz\, J_{gx}(x_{i+1},y,z,t)$$

$$= -D_g^{i,j,k}(t)\,\frac{\dfrac{1}{h_y^j h_z^k}\displaystyle\int_{h_y^j} dy \int_{h_z^k} dz\, \phi_g(x_{i+1},y,z,t) - \bar{\bar{\phi}}_g^{i,j,k}(t)}{h_x^i/2}$$

$$= -D_g^{i+1,j,k}(t)\,\frac{\bar{\bar{\phi}}_g^{i+1,j,k}(t) - \dfrac{1}{h_y^j h_z^k}\displaystyle\int_{h_y^j} dy \int_{h_z^k} dz\, \phi_g(x_{i+1},y,z,t)}{h_x^{i+1}/2} \quad (3)$$

where the integrated term is the surface-averaged flux at x_{i+1}.

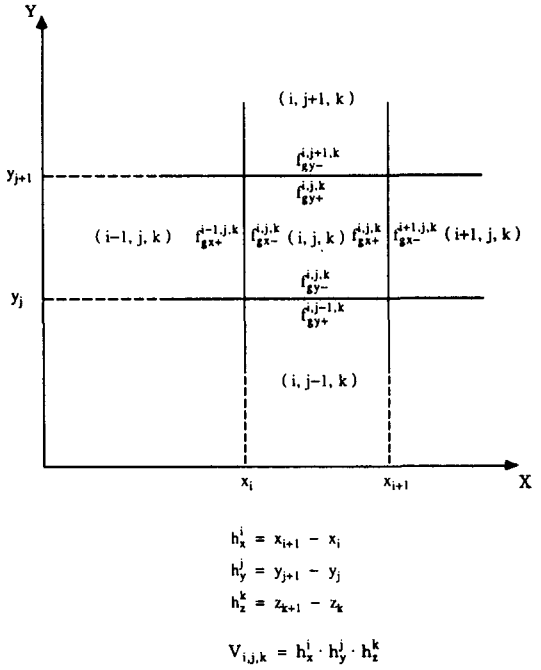

$$h_x^i = x_{i+1} - x_i$$

$$h_y^j = y_{j+1} - y_j$$

$$h_z^k = z_{k+1} - z_k$$

$$V_{i,j,k} = h_x^i \cdot h_y^j \cdot h_z^k$$

Fig. 1. Notation for Specifying Two-Dimensional Correction Factors

The remaining five surface-averaged net currents can be expressed in analogy with equation (3). The elimination of the surface-averaged flux from the two expressions in equation (3), then, yields the surface-averaged net current in terms of known quantities and the volume-averaged fluxes. However equation (3) can be a poor approximation for larger mesh sizes. A way of getting around this problem is to alter equation (3) so that it is forced to be exact. By introducing correction factors [6,7,8] into equation (3) and dividing the surface-averaged flux by these factors, we can rewrite equation (3) as

$$\int_{h_y^j} dy \int_{h_z^k} dz\, J_{gx}(x_{i+1},y,z,t)$$

$$= -D_g^{i,j,k}(t)\,\frac{\dfrac{1}{f_{gx+}^{i,j,k}(t)}\displaystyle\int_{h_y^j} dy \int_{h_z^k} dz\, \phi_g(x_{i+1},y,z,t) - h_y^j h_z^k \bar{\bar{\phi}}_g^{i,j,k}(t)}{h_x^i/2}$$

$$= -D_g^{i+1,j,k}(t)\,\frac{h_y^j h_z^k \bar{\bar{\phi}}_g^{i+1,j,k}(t) - \dfrac{1}{f_{gx-}^{i+1,j,k}(t)}\displaystyle\int_{h_y^j} dy \int_{h_z^k} dz\, \phi_g(x_{i+1},y,z,t)}{h_x^{i+1}/2} \quad (4)$$

where, $f_{gx+}^{i,j,k}(t) \equiv \dfrac{\displaystyle\int_{h_y^j} dy \int_{h_z^k} dz\, \phi_g(x_{i+1},y,z,t)}{\displaystyle\int_{h_y^j} dy \int_{h_z^k} dz\, \phi_g^{hom}(x_{i+1}^-,y,z,t)}$

$$f_{gx-}^{i+1,j,k}(t) \equiv \frac{\displaystyle\int_{h_y^j} dy \int_{h_z^k} dz\, \phi_g(x_{i+1},y,z,t)}{\displaystyle\int_{h_y^j} dy \int_{h_z^k} dz\, \phi_g^{hom}(x_{i+1}^+,y,z,t)}$$

$f_{gx+}^{i,j,k}(t)$, $f_{gx-}^{i+1,j,k}(t)$ = correction factors,

$\phi_g^{hom}(x_{i+1}^{\pm},y,z,t)$ = homogeneous surface fluxes on both sides of x_{i+1}

And analogous expressions can be written for the five other surfaces. In equation (4), $\phi_g(x_{i+1},y,z,t)$ is the physically real, heterogeneous flux at an arbitrary surface x_{i+1} which is continuous everywhere in the reactor core region. The fictitious homogenized fluxes, $\phi_g^{hom}(x_{i+1}^{\pm},y,z,t)$ at surface x_{i+1}, are viewed as arising when homogenized diffusion theory parameters are used throughout the nodes. The ϕ_g^{hom}'s are thus allowed to be discontinuous across the surface. For this reason, the correction

factors are referred to as "discontinuity factors" and have no particular physical significance. In general, $f_{gx-}^{i+1,j,k}(t) \neq f_{gx+}^{i,j,k}(t)$. Note that the correction factors(f's) account for the fact that we are assuming Fick's law with a somewhat arbitrary value of D_g to be correct and for the fact that we are making the finite-difference approximations. Equation (4) can now be solved for the surface-averaged net current at x_{i+1} by eliminating the physically real continuous surface-averaged flux. The following relationship is thus obtained.

$$\int_{h_y^j} dy \int_{h_z^k} dz\, J_{gx}(x_{i+1},y,z,t)$$

$$= -h_y^j h_z^k \left[\frac{h_x^i f_{gx+}^{i,j,k}(t)}{2 D_g^{i,j,k}(t)} \right.$$

$$\left. + \frac{h_x^{i+1} f_{gx-}^{i+1,j,k}(t)}{2 D_g^{i+1,j,k}(t)} \right]^{-1} [f_{gx-}^{i+1,j,k}(t) \bar{\phi}_g^{i+1,j,k}(t) - f_{gx+}^{i,j,k}(t) \bar{\phi}_g^{i,j,k}(t)] \quad (5)$$

Similar expressions can be obtained for other five surfaces. On the other hand the time-difference forms of equations (1) and (2) are obtained by discretizing the continuous time domain into a sequence of absolute time values $t_o, t_1, \ldots, t_n, \ldots, t_T$ where t_o and t_T are the initial and final times, respectively. The time dependent quantities can be symbolized by using subscript, n. We then approximate the time derivative for each time interval $\Delta t_n = t_{n+1} - t_n$ as

$$\frac{\partial}{\partial t} F^{i,j,k}(t) \equiv \frac{(F^{i,j,k})_{n+1} - (F^{i,j,k})_n}{\Delta t_n} \quad (6)$$

where $F^{i,j,k}(t)$ represents $\bar{\phi}_g^{i,j,k}$ or $\bar{C}_d^{i,j,k}$.
The delayed neutron precursor terms are central differenced over this time interval as

$$\bar{C}_d^{i,j,k} = \frac{1}{2}[(\bar{C}_d^{i,j,k})_{n+1} + (\bar{C}_d^{i,j,k})_n] \quad (7)$$

By using equations (6) and (7), the implicit form of the equation (2) can be written as

$$\frac{[(\bar{C}_d^{i,j,k})_{n+1} - (\bar{C}_d^{i,j,k})_n]}{\Delta t_n} = \beta_d \left[\sum_{g'=1}^{G} \nu\Sigma_{fg'}^{i,j,k} \bar{\phi}_{g'}^{i,j,k} \right]_{n+1}$$

$$- \lambda_d \left[\frac{(\bar{C}_d^{i,j,k})_{n+1} + (\bar{C}_d^{i,j,k})_n}{2} \right] \quad (8)$$

Equation (8) can be rearranged to obtain

$$(\bar{C}_d^{i,j,k})_{n+1} = \left(\frac{1 - \frac{\lambda_d}{2}\Delta t_n}{1 + \frac{\lambda_d}{2}\Delta t_n} \right) (\bar{C}_d^{i,j,k})_n + B_d^n \Delta t_n \left[\sum_{g'=1}^{G} \nu\Sigma_{fg'}^{i,j,k} \bar{\phi}_{g'}^{i,j,k} \right]_{n+1} \quad (9)$$

where, $B_d^n = \dfrac{\beta_d}{1 + \frac{\lambda_d}{2}\Delta t_n}$

By using equations (6), (7), and (9) and by substituting of equation (5) and analogous expressions for the five other surface-averaged net currents for node (i,j,k) into equation (1), we can obtain the following set of finite-difference equations :

$$\frac{V_{i,j,k}}{v_g} \frac{(\bar{\phi}_g^{i,j,k})_{n+1} - (\bar{\phi}_g^{i,j,k})_n}{\Delta t_n}$$

$$= -h_y^j h_z^k \left[\frac{h_x^i f_{gx+}^{i,j,k}}{2 D_g^{i,j,k}} + \frac{h_x^{i+1} f_{gx-}^{i+1,j,k}}{2 D_g^{i+1,j,k}} \right]_{n+1}^{-1} [f_{gx-}^{i+1,j,k} \bar{\phi}_g^{i+1,j,k} - f_{gx+}^{i,j,k} \bar{\phi}_g^{i,j,k}]_{n+1}$$

$$-h_y^j h_z^k \left[\frac{h_x^i f_{gx-}^{i,j,k}}{2 D_g^{i,j,k}} + \frac{h_x^{i-1} f_{gx+}^{i-1,j,k}}{2 D_g^{i-1,j,k}} \right]_{n+1}^{-1} [f_{gx+}^{i-1,j,k} \bar{\phi}_g^{i-1,j,k} - f_{gx-}^{i,j,k} \bar{\phi}_g^{i,j,k}]_{n+1}$$

$$-h_x^i h_z^k \left[\frac{h_y^j f_{gy+}^{i,j,k}}{2 D_g^{i,j,k}} + \frac{h_y^{j+1} f_{gy-}^{i,j+1,k}}{2 D_g^{i,j+1,k}} \right]_{n+1}^{-1} [f_{gy-}^{i,j+1,k} \bar{\phi}_g^{i,j+1,k} - f_{gy+}^{i,j,k} \bar{\phi}_g^{i,j,k}]_{n+1}$$

$$-h_x^i h_z^k \left[\frac{h_y^j f_{gy-}^{i,j,k}}{2 D_g^{i,j,k}} + \frac{h_y^{j-1} f_{gy+}^{i,j-1,k}}{2 D_g^{i,j-1,k}} \right]_{n+1}^{-1} [f_{gy+}^{i,j-1,k} \bar{\phi}_g^{i,j-1,k} - f_{gy-}^{i,j,k} \bar{\phi}_g^{i,j,k}]_{n+1}$$

$$-h_x^i h_y^j \left[\frac{h_z^k f_{gz+}^{i,j,k}}{2 D_g^{i,j,k}} + \frac{h_z^{k+1} f_{gz-}^{i,j,k+1}}{2 D_g^{i,j,k+1}} \right]_{n+1}^{-1} [f_{gz-}^{i,j,k+1} \bar{\phi}_g^{i,j,k+1} - f_{gz+}^{i,j,k} \bar{\phi}_g^{i,j,k}]_{n+1}$$

$$-h_x^i h_y^j \left[\frac{h_z^k f_{gz-}^{i,j,k}}{2 D_g^{i,j,k}} + \frac{h_z^{k-1} f_{gz+}^{i,j,k-1}}{2 D_g^{i,j,k-1}} \right]_{n+1}^{-1} [f_{gz+}^{i,j,k-1} \bar{\phi}_g^{i,j,k-1} - f_{gz-}^{i,j,k} \bar{\phi}_g^{i,j,k}]_{n+1}$$

$$- V_{i,j,k} [\Sigma_g^{i,j,k} \bar{\phi}_g^{i,j,k}]_{n+1} + V_{i,j,k} \left[\sum_{g'=1}^{G} \chi_g (1-\beta)\, \nu\Sigma_{fg'}^{i,j,k} \bar{\phi}_{g'}^{i,j,k} \right]_{n+1}$$

$$+ V_{i,j,k} \left[\sum_{g' \neq g} \Sigma_{gg'}^{i,j,k} \bar{\phi}_{g'}^{i,j,k} \right]_{n+1}$$

$$+ \sum_{d=1}^{DG} \frac{\lambda_d}{2} \left[\frac{2}{\lambda_d} (\bar{C}_d^{i,j,k})_n + B_d^n \Delta t_n \left\{ \sum_{g'=1}^{G} \nu\Sigma_{fg'}^{i,j,k} \bar{\phi}_{g'}^{i,j,k} \right\} \right]_{n+1} \quad (10)$$

Since all transient problems are assumed to start

from a steady state condition, the initial precursor density terms at node (i,j,k) are calculated by the steady state relation

$$(\bar{\bar{C}}_d^{i,j,k})_o = \frac{\beta_d}{\lambda_d}\left[\sum_{g=1}^{G} \nu\Sigma_{fg}^{i,j,k}\,\bar{\bar{\phi}}_g^{i,j,k}\right]_o \tag{11}$$

2.2. Boundary Conditions

For the interfaces not on the problem boundary, the surface-averaged currents are continuous across the boundary between two neighbouring nodes. Along the exterior boundary of the reactor, the surface-averaged flux is considered as constant according to problem situations characteristics.

2.3. Estimation of the Discontinuity Factors

Prior to examination of the coarse-mesh steady state and transient solutions using the method developed in Section 2.1, the discontinuity factors should be known in advance. As was mentioned in Section 1, these factors can be calculated by the fine-mesh finite-difference method, NEM, ANM, or other methods. The discontinuity factors are then used to get the initial coarse mesh solution for the steady state condition.

By using equation (6), the factor $f_{gx+}^{i,j,k}$ at steady state condition as shown in Figure 1 is given by

$$[f_{gx+}^{i,j,k}]_o = \left[\frac{\bar{\phi}_{gx+}^{i,j,k}}{\bar{\bar{\phi}}_g^{i,j,k} - \frac{h_x^i}{2D_g^{i,j,k}}\bar{J}_{gx+}^{i,j,k}}\right]_o \tag{12}$$

where

$\bar{\phi}_{gx+}^{i,j,k}$ = surface-averaged flux at surface x_{i+1} of node (i,j,k),

$\bar{J}_{gx+}^{i,j,k}$ = surface-averaged net current at surface x_{i+1} of node (i,j,k).

Analogous calculations can be performed for the other remaining surfaces of node (i,j,k). In equation (12), $\bar{\phi}_{gx+}^{i,j,k}$ is a heterogenous flux at arbitrary surface x_{i+1} as shown in Figure 1 and the same as $\bar{\phi}_{gx-}^{i+1,j,k}$

Once surface-averaged flux and current, and node-averaged flux are obtained, the discontinuity factors for the initial and coarse-mesh steady state conditions can be determined by equation (12).

In this study the initial discontinuity factors are calculated from the fine-mesh finite difference method. In the method, by using equation (10) at steady state by setting all discontinuity factors to unity, surface-averaged flux and current, and node-averaged flux can easily be obtained using the continuity condition of the neutron flux and current at the node interface.

Once the initial discontinuity factors are determined, the coarse-mesh steady state and transient core calculations, according to the method developed in Section 2.1, are continuously performed based on the factors. Therefore accuracy of the initial values greatly affects the entire calculational accuracy.

In order to update efficiently the discontinuity factors with time, we assume that the surface-averaged flux, $\bar{\phi}_{gx+}^{i,j,k}$ does not vary within a very small time interval(Δt). By using Eq. (4), therefore, $f_{gx}^{i,j,k}$ for the transient is approximated as follows

$$[f_{gx+}^{i,j,k}]_{n+1} = \frac{[\bar{\phi}_{gx+}^{i,j,k}]_{n+1}}{\left[\bar{\bar{\phi}}_g^{i,j,k} - \frac{h_x^i}{2D_g^{i,j,k}}\bar{J}_{gx+}^{i,j,k}\right]_{n+1}} = \frac{[\bar{\phi}_{gx+}^{i,j,k}]_n}{\left[\bar{\bar{\phi}}_g^{i,j,k} - \frac{h_x^i}{2D_g^{i,j,k}}\bar{J}_{gx+}^{i,j,k}\right]_{n+1}} \tag{13}$$

In other remaining faces, the discontinuity factors are calculated in the same manner.

3. Application to Two-Dimensional Reactor Problems

3.1. Benchmark Problems

-TWIGL Reactor Problem

The TWIGL test problem[9,10] is a simplified reactor kinetics model as shown in Figure 2. The problem is modeled with two neutron energy groups, one delayed precursor group, and quarter-core symmetry. The reactor has a three region core containing 400 fuel elements with widths of 8 cm. The two-group constants for the problem and transient situations are given in Table 1. Two transients are initiated either by decreasing the absorption cross section in region 1 of Figure 2 by 0.0035 cm^{-1} either as a step perturbation or as a ramp perturbation in 0.2 seconds. Each transient is calculated for 0.5 seconds.

-LRA Problem

The LRA benchmark problem[10,11,12] is a full-core BWR kinetics problem with two neutron energy groups and two delayed neutron precursor families. A superprompt critical transient from low power is induced by the rapid withdrawal of an asymmetric peripheral control rod. A simple Doppler feedback mechanism is built-in in this problem. The feedback model is specified by two relations :

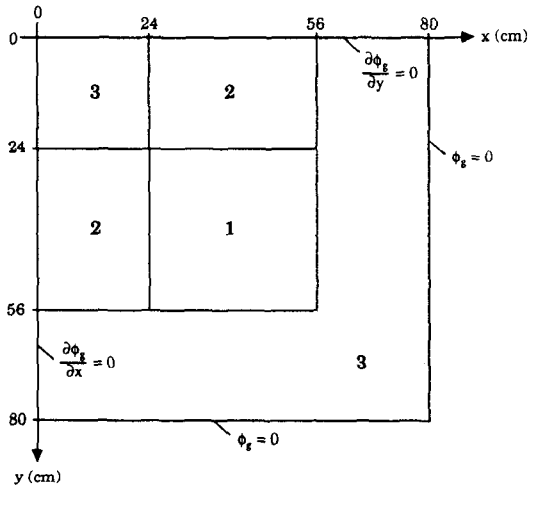

Fig. 2. One Quadrant of the Core for the Two-Dimensional TWIGL Benchmark

adiabatic heatup :

$$\frac{\partial}{\partial t}T(\vec{r},t) = \alpha\,[\,\Sigma_{f1}(\vec{r},t)\,\phi_1(\vec{r},t) + \Sigma_{f2}(\vec{r},t)\,\phi_2(\vec{r},t)]$$

and Doppler feedback :

$$\Sigma_{a1}(\vec{r},t) = \Sigma_{a1}(\vec{r},0)\left[\,1+\gamma\left(\sqrt{T(\vec{r},t)}-\sqrt{T_o}\right)\right]$$

where α, γ, and T_o are known constants.

The reactor has 312 fuel elements, each having a width of 15 cm. The core is reflected by 30 cm of pure water. To make computations more economical, this problem has been contracted into a quarter-core problem, maintaining the same characteristics of the original problem. Figure 3 shows a horizontal cross section of a reactor quadrant, consisting of 5 regions : fuel type I with rod (1), fuel type I without rod (2), fuel type II with rod (3), fuel type II without rod (4), and reflector (5). The group constants of 5 regions and transient

Table 1. Group Constants for TWIGL Problem

Region	Group	Dg (cm)	Σ_{ag} (cm^{-1})	$\nu\Sigma_{fg}$ (cm^{-1})	Σ_{21} (cm^{-1})
1	1	1.4	0.01	0.007	0.01
	2	0.4	0.15	0.2	
2	1	1.4	0.01	0.007	0.01
	2	0.4	0.15	0.2	
3	1	1.3	0.008	0.003	0.01
	2	0.5	0.06	0.06	

Transient 1

Step perturbation in region 1 :

$\Delta\Sigma_{a2} = -0.0035\ cm^{-1}$ $\quad t=0$

The transient is calculated for 0.5 seconds.

Transient 2

Ramp perturbation in region 1 :

$\Delta\Sigma_{a2}(t) = 0.15[1-0.1166667\ t]\ cm^{-1}$

$t \leq 0.2$ seconds

$0.1465\ cm^{-1}$

$t \geq 0.2$ seconds

The transient is calculated for 0.5 seconds.

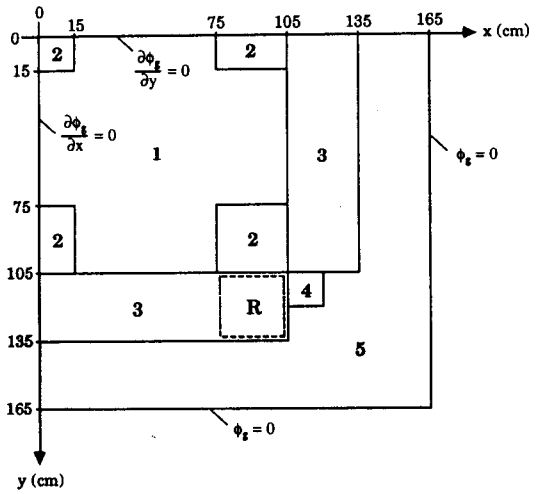

Fig. 3. One Quadrant of the Core for the Two -Dimensional LRA Benchmark

Table 2. Group Constants for TWIGL Problem

Region	Group	Dg (cm)	Σ_{ag} (cm^{-1})	$\nu\Sigma_{fg}$ (cm^{-1})	Σ_{21} (cm^{-1})
1	1	1.255	0.008252	0.004602	0.02533
	2	0.211	0.1003	0.1091	
2	1	1.268	0.007181	0.004609	0.02767
	2	0.1902	0.07047	0.08675	
3, R	1	1.259	0.008002	0.004663	0.02617
	2	0.2091	0.08344	0.1021	
4	1	1.259	0.008002	0.004663	0.02617
	2	0.2091	0.073324	0.1021	
5	1	1.257	0.0006034	0.0	0.04754
	2	0.1592	0.01911	0.0	

Perturbation

Control rod region (R) is given by

$\Delta\Sigma_{a2} = 0.08344(1-0.0606184\ t)\ cm^{-1}$

for $t \leq 2.0$ seconds

$0.073324\ cm^{-1}$

for $t \geq 2.0$ seconds

The transient is calculated for 3.0 seconds.

situations are shown in Table 2.

3.2. Computer Code

In order to perform the numerical analysis the equivalent nodal finite-difference equation developed in Section 2 has been incorporated into a computer program, TRANDIS(program to solve TRANsient problems using DIScontinuity factors). TRANDIS is written in standard FORTRAN 77. All calculations presented in next section are performed in single precision on IBM 386/PC and CYBER 170/875. TRANDIS solves two -dimensional, two-group problems and is capable of handling uniform mesh spacing and rectangular geometry. TRANDIS can also be easily extended to three dimension and multi-group problems.

For the benchmark problems shown above, we assume that the surface discontinuity factors at the symmetry line with zero net current boundary conditions are the same as in the previous time step and the factors at the core outer line with zero surface-averaged fluxes are equal to unity.

3.3. Numerical Results and Discussions

-TWIGL Reactor Problem

All the calculations for the TWIGL reactor problem were performed using one node per fuel element and classified to two stages : steady state and transient calculations. The steady state calculation results include the eigenvalue and the nodal power distributions to compare with the references. The comparison of the eigenvalue with the reference solution[10] at steady state is given as follows

Reference ; 0.91318, TRANDIS ; 0.913155

The comparison of the nodal power distributions obtained from TRANDIS with the reference[10] is also shown in Figure 4. The absolute mean error in the nodal power is 0.2%. The maximum relative error of 1.1% occurs at the core periphery node, where the relative power is very low. During the transient, the results of the mean power densities are summarized in Table 3 and the nodal

Table 3. Average Power Density for the TWIGL Benchmark

Time	Ramp-Perturbation			Step-Perturbation		
(sec)	Reference[a]	TRANDIS[b]	Difference[c](%)	Reference[a]	TRANDIS[d]	Difference[c](%)
0.00	1.000	1.000	–	1.000	1.000	–
0.05	1.131	1.112	1.68	2.065	2.031	1.65
0.10	1.316	1.294	1.67	2.081	2.066	0.72
0.15	1.577	1.551	1.65	2.086	2.085	0.14
0.20	1.972	1.941	1.57	2.096	2.097	−0.05
0.25	2.082	2.077	0.24	2.104	2.108	−0.19
0.30	2.090	2.099	−0.43	2.111	2.117	−0.28
0.35	2.098	2.109	−0.52	2.117	2.126	−0.43
0.40	2.105	2.118	−0.62	2.124	2.136	−0.56
0.45	2.113	2.128	−0.71	2.132	2.145	−0.61
0.50	2.122	2.137	−0.71	2.141	2.154	−0.61

a. Calculation results by fine-mesh NEM (Ref. [10])

b. Time step ; 1 msec, Flux convergence criteria ; 10^{-4}, Execution time (IBM 386/PC) ; 118 sec

c. $\text{Difference} = \dfrac{(\text{Reference}-\text{TRANDIS})}{\text{Reference}} \times 100$

d. Time step ; 2.5msec, Flux convergence criteria ; 10^{-4}, Execution time (IBM 386/PC) ; 52 sec

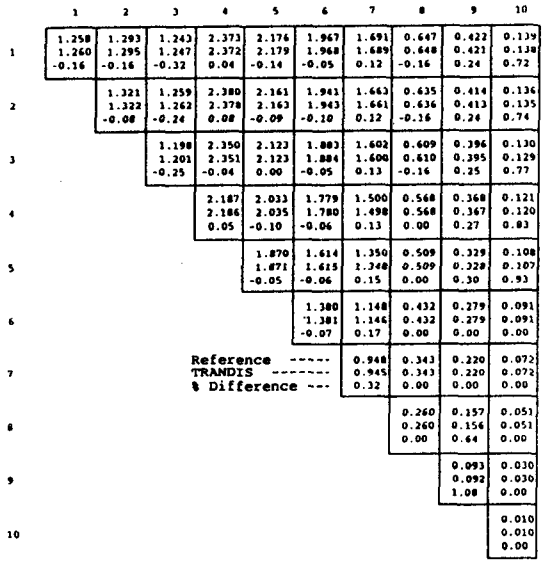

Fig. 4. Node-Averaged Power Distribution for TWIGL at Steady State

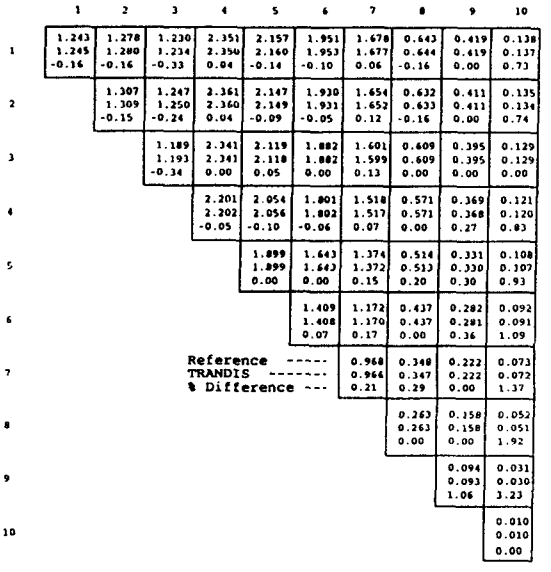

Fig. 5a. Node-Averaged Power Distribution for TWIGL with Ramp-Perturbation at 0.1 sec.

power distributions at 0.1 and 0.5 seconds are shown in Figure 5, respectively. The maximum error in the mean power density is about 1.68% in the ramp perturbation and about 1.65% in the

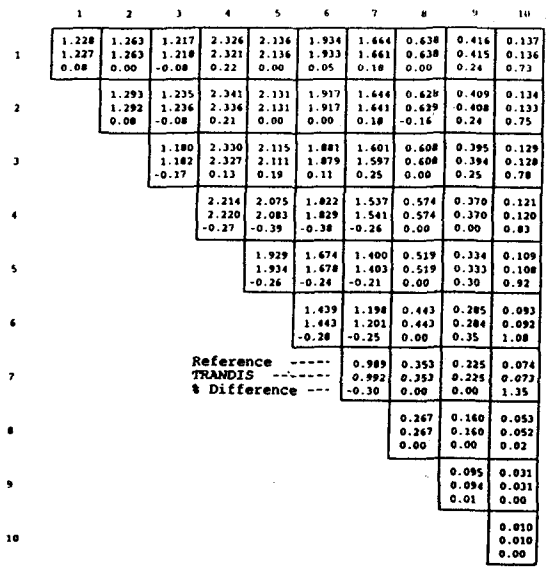

Fig. 5b. Node-Averaged Power Distribution for TWIGL with Ramp-Pertubation at 0.5 sec.

step perturbation. In addition the maximum error in the assemblywise power distribution is less than 0.4% in the inner and 3.2% in the outer cores where the relative powers are very low. These results indicate that the TRANDIS solution is accurate. The TWIGL reactor problem demonstrates that the nodal method with equivalent finite-difference discontinuity factors can obtain accurate transient solutions with coarse spatial and temperal meshes.

-LRA Benchmark Problem

All the calculations for LRA were performed using one node per fuel element (15 cm×15 cm) and classified to two stages as TWIGL problem. A comparison of the nodal static power distributions with the reference[11] is given in Figure 6. The maximum difference in nodal power is less than 2.0%. Figure 7 compares the mean powers for the reference solution and the TRANDIS over the interval $0 \leq t \leq 3.0$ seconds. This figure shows that TRANDIS predict the transient behaviors accurately.

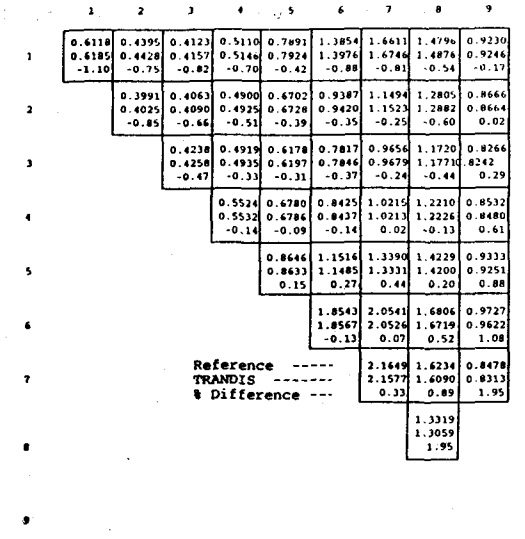

Fig. 6. Node-Averaged Power Distribution for LRA at Steady State

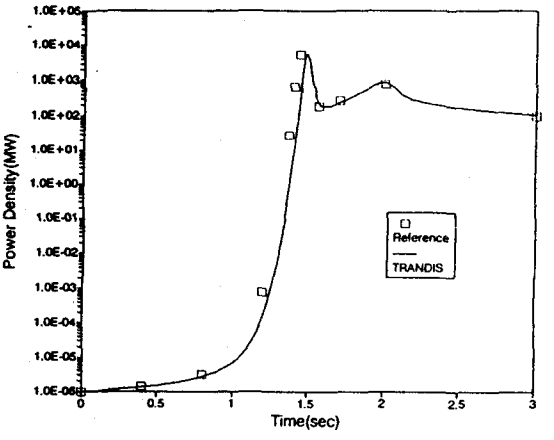

Fig. 7. Average Power Densities vs. Time for LRA Benchmark

A summary of transient results based on several different methods is given in Table 4. It shows that TRANDIS calculations with coarse spatial and temperal meshes and matrix updating with surface-averaged discontinuity factors are accurate and very computationally efficient. TRANDIS solution slightly overpredicts peak powers and temperatures. The time to the first power peak is slightly delayed compared to other methods. The execu-

Table 4. Comparison of Results for LRA 2D Test Problem

	Werner[1] (CUBBOX)	Finnemann[2] (IQSBOX)	Sims[3]	Shober[4]	Smith[5] (QUANDRY)	Christe-nsen[10]	TRANDIS	Refere-nce[11]
Initial Eigenvalue	0.99633	0.99631	-	0.99655	0.99641	0.99619	0.99637	0.99636
Number of Time Steps	1200	522	1300	1000	1000	-	680	2600
CPU Time (sec) (Computer)	180 IBM360/91	255 CYBER 175	1014 IBM370 /168	210 IBM370 /168	307 IBM370 /168	26473 Burroughs B7800	138(*) CYBER 170/875	1661 IBM370 /195
Time to first peak (sec)	1.421	1.455	1.432	1.426	1.435	1.500	1.482	1.436
Power at first peak (MW)	5734	5451	5760	5552	5473	7447	5724	5411
Time to second peak (sec)	2.0	2.0	2.0	2.0	2.0	2.0	2.0	2.0
Power at second peak (MW)	~830	~800	840	815	797	1098	828	784
Average Temp. at 3.0 sec (°K)	1070	1127	1142	1127	1108	-	1085	10.87
Maximum Temp. at 3.0 sec (°K)	2925	2989	3163	3112	3029	-	3058	2948
Power at 3.0 sec (MW)	~60	~100	-	97.0	97.5	74.1	104.5	96.2

(*) Computing time in IBM386/PC is 397 seconds.

tion time for TRANDIS compares well with those of CUBBOX, IQSBOX, QUANDRY and so on.

A comparison of the nodal transient power distributions with the reference case is not shown in this paper since it is not convenient to compare each other due to the differences of the mean power densities at each time.

4. Conclusions

The test problem results shown in the study demonstrate that the new method using the discontinuity factors equivalent to the finite-difference method for the transient problems, which is developed in Section 2, is shown to be accurate and highly efficient. It is found that if LWR's can be homogenized into assembly-sized nodes, this new method can be expected to yield assembly-averaged powers accurate to within approximately two percent, static reactor eigenvalues accurate to within about 0.002 percent, and average power densities versus time to give very similar values to the references in trend and magnitude. This method is also shown to be more computationally efficient than several different methods of current interest.

Prior to the application of this method on test problems, it is necessary to guess accurate initial values of node-averaged and surface-averaged fluxes through the fine-mesh calculation at a

steady state condition. Therefore, the study to get not only accurately but efficiently the initial values can be performed using several methods such as ANM, NEM, or the finite-difference method with one quadrant assembly-sized(or finer) nodes.

It is desirable for reducing much of execution time to adopt the temporal integration scheme for the use of larger time steps and to develop an acceleration scheme which is more computationally efficient than the conventional two-group iterative scheme.

References

[1] S. Langenbuch, W. Maurer, W. Werner, "Coarse-Mesh Flux Expansion Method for the Analysis of Space-Time Effects in Large Light-Water Reactor Cores," Nucl. Sci. Eng., **63**, 437 (1977).

[2] H. Finnemann, F. Bennewitz, M.R. Wagner, "Interface Current Techniques for Multidimensional Reactor Calculations," Atomkernenergie, **30**(2), 123 (1977).

[3] R. Sims and A.F. Henry, "Coarse Mesh Nodal Method Based on Response Matrix Considerations," Trans. Am. Nucl. Soc., **24**, 193 (1976).

[4] R.A. Shober, "A Nodal Method for Solving Transient Fewgroup Neutron Diffusion Equations," ANL-78-51, June 1978.

[5] K.S. Smith, "An Analytic Nodal Method for Solving the Two-Group, Multidimensional, Static and Transient Neutron Diffusion Equations," MS Thesis, Dept. of Nuclear Engineering, MIT, Cambridge, MA, March 1979.

[6] K. Koebke, "A New Approach to Homogenization and Group Condensation," Paper Presented at the IAEA Technical Committee on Homogenization Methods in Reactor Physics, Lugano, Switzerland, November 1978.

[7] K.S. Smith, "Spatial Homogenization Methods for Light Water Reactor Analysis," Ph.D Thesis, Dept. of Nuclear Engineering, MIT, Cambridge, MA, June 1980.

[8] M.H. Chang, "The Application of Nodal Methods to the Transport Equation," Ph.D. Thesis, Dept. of Nuclear Engineering, MIT, Cambridge, MA, October 1984.

[9] L.A. Hageman and J.B. Yasinsky, "Comparison of Alternating-Direction Time-Differencing Methods and Other Implicit Methods for the Solution of the Neutron Group Diffusion Equations," Nucl. Sci. Eng., **38**, 8 (1969).

[10] B. Christensen, "Three-Dimensional Static and Dynamic Reactor Calculations by the Nodal Expansion Method," Riso-R-496, Denmark, May 1985.

[11] Argonne Code Center : Benchmark Problem Book, ANL-7416, Suppl. II, June 1977.

[12] P.S. Christensen, F.J. Fayers, S. Langenbuch, F.N. McDonnell, A. Schmidt, E. Vincenti, H. Yoshikawa, and W. Werner, "Survey of the Results of a Two- and Three-Dimensional Kinetics Benchmark Problem Typical for a Thermal Reactor," Proc. Joint NEACRP/CSNI Specialists' Meeting on New Developments in Three-Dimensional Neutron Kinetics and Review of Kinetics Benchmark Calculations, 413 (1975).